Mining Science, vol. 29, 2022, 141–163

www.miningscience.pwr.edu.pl

Mining Science

(Previously Prace Naukowe Instytutu Gornictwa Politechniki Wroclawskiej, ISSN 0370-0798)

ISSN 2300-9586 (print)
ISSN 2353-5423 (online)

Received January 30, 2022; Reviewed; Accepted September 21, 2022

SLOPE REINFORCEMENT DESIGN BASED ON GEOSTUDIO AND FLAC3D

Rongxia YU[1], Zhian HUANG[1, 2], Zhiquan YANG[3]*

[1] State Key Laboratory of High-Efficient Mining and Safety of Metal Mines (University of Science and Technology Beijing), Ministry of Education, Beijing, China

[2] Work Safety Key Lab on Prevention and Control of Gas and Roof Disasters for Southern Coal Mines (Hunan University of Science and Technology), Xiangta, China

[3] Kunming University of Science and Technology, Faculty of Public Safety and Emergency Management, Kunming, China

Abstract: Slope stability of open pit mines has been a hot issue of economic and safety concern. In order to reduce the accidental casualties caused by slope instability, targeted reinforcement solutions should be proposed for them. In this paper, GeoStudio and FLAC3D software were used to model the slope an open pit mine. The safety factors of the slope under natural, rainfall and seismic conditions are analyzed in turn. Additionally, the safety factors derived from different algorithms are compared to mutually verify the reliability of the slope stability analysis. Two sets of reinforcement design solutions – anchor rod and anti-slip pile – are proposed. Then, the two solutions are optimized so that the safety factors of the slope under three conditions reach 1.3, 1.2 and 1.1, respectively, and the optimal solution is selected from the two solutions by combining the economic benefits. The results show that the optimized anchor and anti-slide pile reinforcement solutions result in the safety factors of the slope under different conditions, reaching 1.441, 1.258, and 1.324 and 1.4, 1.238, and 1.23, respectively. The anti-slide pile reinforcement solution is more economical than the anchor reinforcement solution, so it is recommended that the anti-slide pile reinforcement solution should be chosen as the final solution.

***Keywords*:** *opencast mining slope, stability analysis, numerical simulation, reinforcement design*

* Corresponding author: y15269572520@sina.com (Zhiquan Yang)

doi: 10.37190/msc222909

1. INTRODUCTION

In order to meet the growing energy demand of the country, a large number of coal resources have been developed and utilized, and many large surface mines have gradually entered the stage of deep recess mining or underground mining (Xiaoming 2010). Due to the complex geological conditions of the mine site, together with the influence of engineering disturbances and environmental factors, the slope stability problem has been restricting the economic development of the mine. From the perspective of profit maximization, the larger the slope angle of open pit mines and the smaller the stripping ratio, the higher the economic benefits, but the steeper the slope, which can directly cause loss of life and property (Verma et al. 2011). The problem of slope stability has been addressed by scholars in various fields, and research methods in this field have matured, coming to include the limit equilibrium method, the numerical analysis method, and the limit analysis method (DENG 2021; Azmoon et al. 2021).

On the basis of static equilibrium, the limit equilibrium method divides the rock and soil masses into a number of slices, constructs a balance equation for each slice, and then determines the balance relationship of the whole slope in order to derive the safety factor (Kainthola et al. 2013). This family of methods includes the Fellenious method (Deng et al. 2016), the Janbu method (Li et al. 2019), the Bishop method (Alejano et al. 2011), the Spencer method (Harabinová 2017), the Sarma method (Kalatehjari et al. 2013), Morgenstern and Price's method (Kumar et al. 2021), etc. Agam et al. (2016) applied Spencer's method and the General Limit Equilibrium method for slices using the Mohr–Coulomb failure criterion in order to perform the comparative analysis of a slope in Kepong, Kuala Lumpur, with the aim of determining the influence of varying parameters values on changes in safety factor. Tutluoglu et al. (2011) accurately determined the dynamic friction angle of a critical weak clay layer beneath a lignite seam using a two-dimensional limit equilibrium method and a three-dimensional finite-difference model.

Numerical analysis methods have become the principal direction of current research by virtue of their speed, accuracy, and ability to simulate slope excavation and support, including the finite element method (Bui et al. 2011; Li et al. 2016), the boundary element method (Yang et al. 2016), the discrete unit method (Coetzee 2017), fast Lagrangian analysis (FLAC) (Fengshan et al. 2016), etc. Vyazmensky A et al. (2010) used finite element and discrete element modeling methods to analyze the development process of block cave-induced step damage in the slope of a large open pit mine. Nian et al. (2012) used an elastoplastic finite element method using strength-reduction techniques to discuss the effects of curvature angle, slope gradient, and convex- and concave-shaped surface geometry on the stability and failure characteristics of slopes under various boundary conditions. Wei et al. (2009) used the strength reduction and limit equilibrium methods to analyze slopes, and found that both methods yielded better safety factors and damage models, but

that the strength reduction method was more sensitive to convergence criteria, boundary conditions, and grid design, making it difficult to determine the limit state. Vishal et al. (2015) studied a surface coal mine slope in Jharia using numerical code Phase^2 based on finite element method to study the stability of two types of slopes.

The soil is considered to be an ideal plastic body when using the limit analysis method. The upper and lower limit theories have been used to derive the range of ultimate bearing capacity and to subsequently conduct stability analysis (Tschuchnigg et al. 2015; Utili 2013). The upper limit theory requires the construction of a reasonable velocity field, at which time the load is the upper load limit; the lower limit theory requires the establishment of an appropriate stress field to ensure that all parts of the soil are able to achieve stress equilibrium, at which time the load is the lower load limit (Leshchinsky et al. 2015). Based on the kinematic theorem of limit analysis, Nadukuru et al. (2013) analyzed the slopes in three dimensions and determined the displacement solutions for slopes under seismic action, which were applied to the three-dimensional damage model of slopes in order to propose a reasonable range of width and slope height ratios for projects such as excavated slopes.

The limit equilibrium method can be used to estimate the safety factor of slopes without considering the initial conditions, but the stress – strain relationship of the soil is excluded. Neverthless, the strength reduction method can be used to obtain information regarding soil stress, displacement, and pore pressure that cannot be obtained using the limit equilibrium method (Faiz et al. 2020; Liu et al. 2015,). The organic combination of these two methods can make the study of slope stability more reliable. However, there are few studies combining the two methods to analyze the stability of open pit slopes in two and three dimensions and to design the slope reinforcement. Therefore, in this study, GeoStudio software based on the limit equilibrium method and FLAC3D software based on the strength reduction method are both used to simulate the slope, analyze the stability of the slope under different conditions (natural, heavy rainfall, earthquake), and propose designs for reinforcement. The optimal reinforcement solution can be obtained by comparing the safety coefficient, slope displacement and stress conditions after reinforcement.

2. FIELD OVERVIEW

2.1. GEOLOGICAL AND ENVIRONMENTAL CONDITIONS

The exposed strata in the area where the slope of the open pit is located are mainly tuffs of the Permian Upper Emeishan Basalt Group ($P_2\beta$), mudstones of the Devonian Middle Haikou Group (D_2h), and sandstones of the Triassic Upper Shezhi Group (T_3s) underlain by mudstones (D_2h). Groundwater types can be divided into two categories: loose rock-

like pore water and clastic rock-like fracture water. The bedrock mountain mostly forms steep hills under the influence of tectonics. The mudstone and sandstone are easy to form differential weathering , and the strong weathering zone is generally several meters thick, resulting in the development of residual slope and colluvial slope.

2.2. PHYSICAL AND MECHANICAL PARAMETERS OF THE GEOTECHNICAL BODY

All kinds of rock and soil mass were sampled and tested to determine the physical and mechanical parameters of the geotechnical bodies, as shown in Table 1.

Table 1. Physical and mechanical parameters of rock and soil mass

Rock-soi body	Gravity [KN/m^3]	Cohesion [KPa]	Internal friction angle [°]	Young modulus [MPa]	Poisson ratio
Silty clay	19	13.5	11.5	25.1	0.3
Peblly soil	20	16	25	10.1	0.25
Gravelly soil	21	30.5	19.7	20	0.27
Sandstone	26.4	200	27	14500	0.2
Mudstone	26	3800	25	2000	0.3

2.3. WORKING CONDITION SETTING

Stability analysis of the slope was performed under different conditions, including (1) natural conditions, (2) rainstorm conditions (93.77 mm/24 h), and (3) seismic condition; according to the data, the earthquake intensity was 9 degrees and the acceleration was 0.30 g.

3. NUMERICAL SIMULATION ANALYSIS OF THE ORIGINAL SLOPE

3.1. ESTABLISHMENT OF THE MODEL

The profile was imported into GeoStudio software in order to establish a two-dimensional model, and the mesh was divided using Rhino6 and imported into FLAC3D to establish a three-dimensional model. The gravity, friction angle and cohesion of the soil were input into the corresponding areas, so as to specify the materials in different areas. The GeoStudio and FLAC3D models established on the basis of the physical and mechanical parameters of the geotechnical body are shown in Figs. 1 and 2.

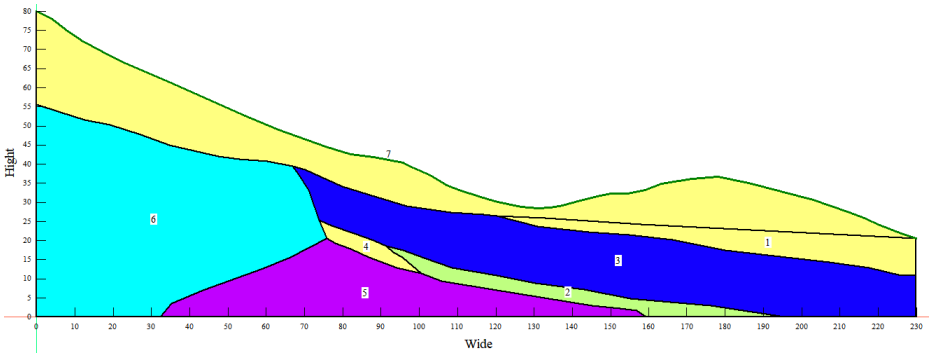

Fig. 1. GeoStudio model

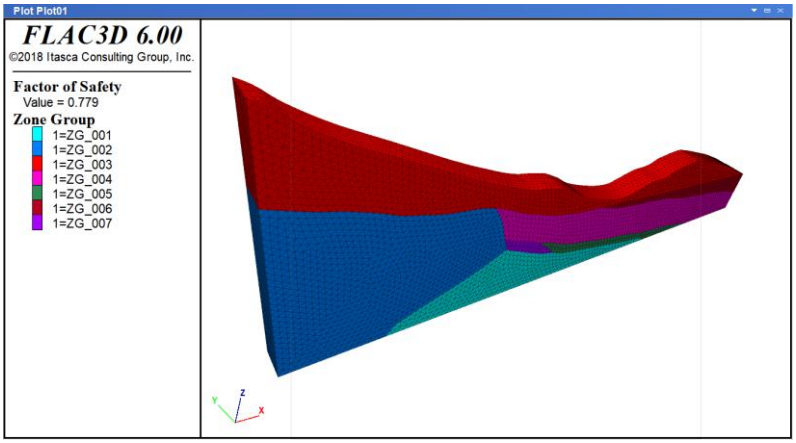

Fig. 2. FLAC3D model

3.2. ANALYSIS OF CALCULATION RESULTS

GeoStudio software, which uses the limit equilibrium method, is able to simulate the slope using the Ordinary method, the Janbu method, the Bishop method, etc., for the purposes of calculating the safety factor and critical slip surface. Meanwhile, the FLAC3D algorithm is based on the strength reduction method, and simulates the slope in three dimensions in order to obtain the safety factor and plastic zone distribution. The two simulation results obtained under different conditions are summarized in Table 2, for the purpose of comparing and analyzing the results obtained using different methods.

Although FLAC3D and GeoStudio use different algorithms, the results of the two algorithms are similar. The results obtained using the Morgenstern–Price method, the Spencer method and the Bishop method are comparable, and are generally large, while the

results obtained using the Janbu method and the Ordinary method are similar, and are, overall, small. The calculation results obtained using the Morgenstern–Price method and the Spencer method under natural and storm conditions are identical, and the results obtained using the Spencer method are closer to the calculation results obtained using the strength reduction method than those obtained using the Morgenstern–Price method under seismic conditions. According to the provisions of the Landslide Prevention Engineering Exploration Code, shown in Table 3, the safety coefficients of the slope under the three working conditions are less than 1; therefore, the slope can be deemed to have been unstable under all three conditions.

Table 2. Summary of slope safety factors under different working conditions

Calculation method	Limit equilibrium method					Strength reduction method
	Morgenstern –Price	Spencer	Bishop	Janbu	Ordinary	
Natural conditions	0.785	0.785	0.787	0.735	0.747	0.777
Rainstorm conditions	0.635	0.635	0.636	0.594	0.604	0.629
Seismic conditions	0.724	0.725	0.726	0.676	0.686	0.736

Table 3. Scale of stability of landslide

Safety factor (Fs)	$Fs < 1.00$	$1.0 \leq Fs < 1.05$	$1.05 \leq Fs < 1.15$	$Fs \leq 1.15$
Stable state	unstable	less stable	basically stable	stable

3.3. ANALYSIS OF SIMULATION RESULTS

3.3.1. SLIP SURFACE ANALYSIS

The simulation results of the slope under the three different conditions were roughly similar, and the safety factor of slope under rainstorm conditions was the lowest, while the risk was the highest. Therefore, the simulation results obtained for the slope under rainstorm conditions were taken as an example for further analysis.

The slip surface simulated by GeoStudio is shown in Fig. 3, and is concentrated in the middle and upper part of the original slope. The height and width of the sliding surface are about 36m and 76m respectively. The distribution of the maximum shear strain increment of the original slope is shown in Fig. 4. There is a plastic zone in the middle and upper part of the slope, and the maximum shear strain increment of this part is significantly larger than that of the surrounding soil. On the left side of the top of the slope, the maximum shear strain increment reaches its maximum value. The slip surfaces

simulated by the two software packages are roughly similar, and the slope is dominated by circular and arc slip surfaces.

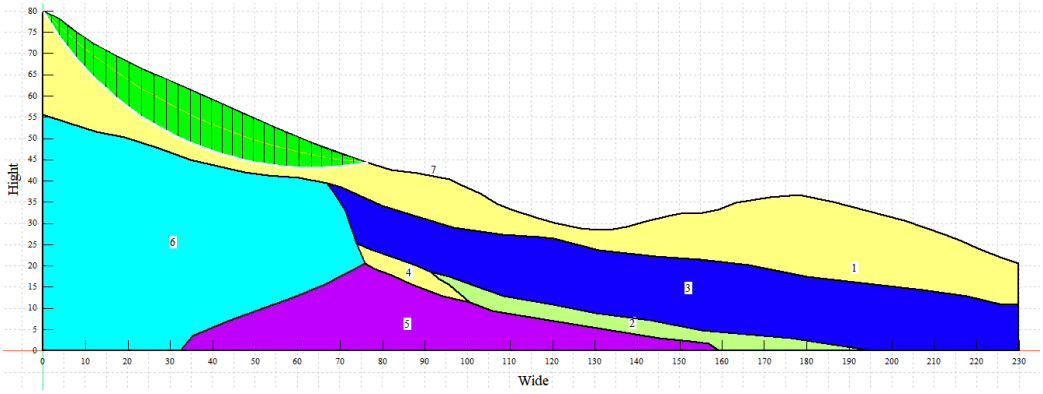

Fig. 3. GeoStudio simulation result

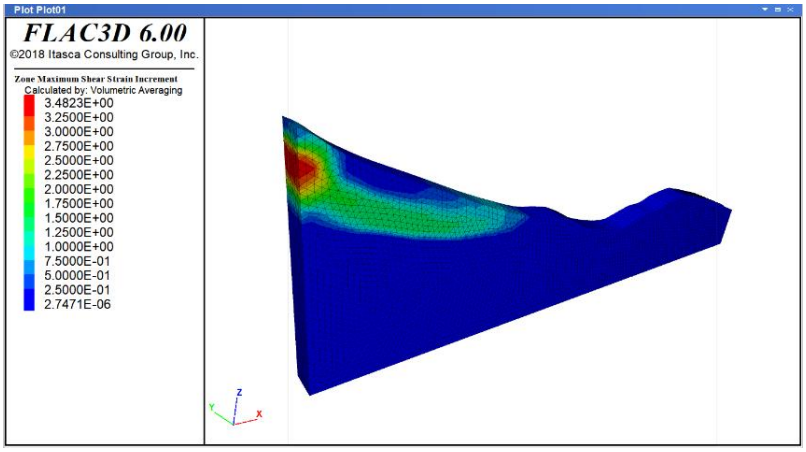

Fig. 4. FLAC3D simulation result

3.3.2. CHARACTERISTICS OF DISPLACEMENT DISTRIBUTION

In order to perform the stability analysis of the slope in multiple respects, the comprehensive displacement of the original slope under rainstorm conditions was extracted, as shown in Fig. 5. There is a sliding surface similar to a circular arc in the middle and upper part of the slope, which is consistent with the simulation results obtained for the plastic zone depicted in Fig. 4. The displacement above the arc is significantly higher than that of the surrounding soil, and the maximum displacement reaches 24.1 m, which is located at the top of the slope.

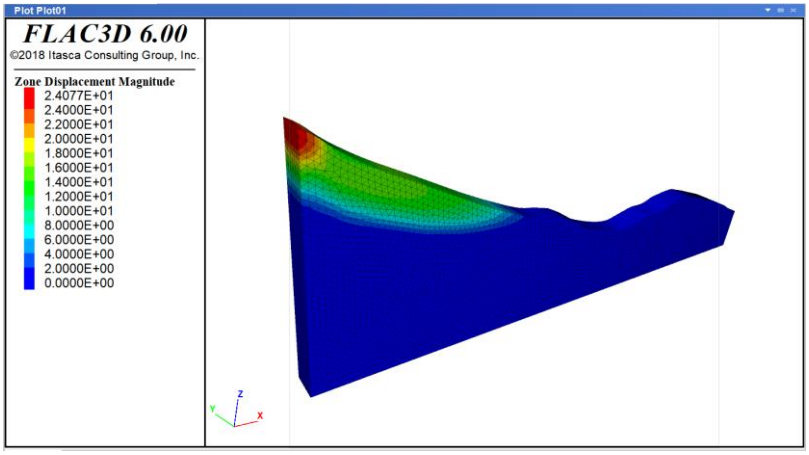

Fig. 5. Displacement distribution map of the original slope

3.3.3. CHARACTERISTICS OF STRESS DISTRIBUTION

The stress distribution in the horizontal direction of the slope under rainstorm conditions is shown in Fig. 6. The horizontal stress mainly consists of compressive stress, which grows with increasing slope depth, and the peak value is located at the bottom of the right side of the slope, reaching 5.37×10^5 Pa.

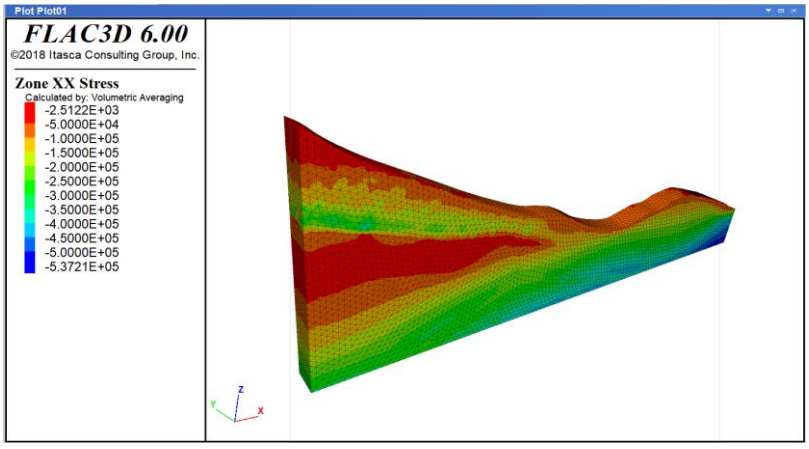

Fig. 6. Original horizontal stress cloud of slope

The vertical stress of the slope is shown in Fig. 7. The compressive stress of the slope shows a hierarchical distribution, and its contour line is parallel to the slope surface. The compressive stress increases with increasing slope depth, reaching a maximum value of 0.68×10^6 Pa at the bottom of slope.

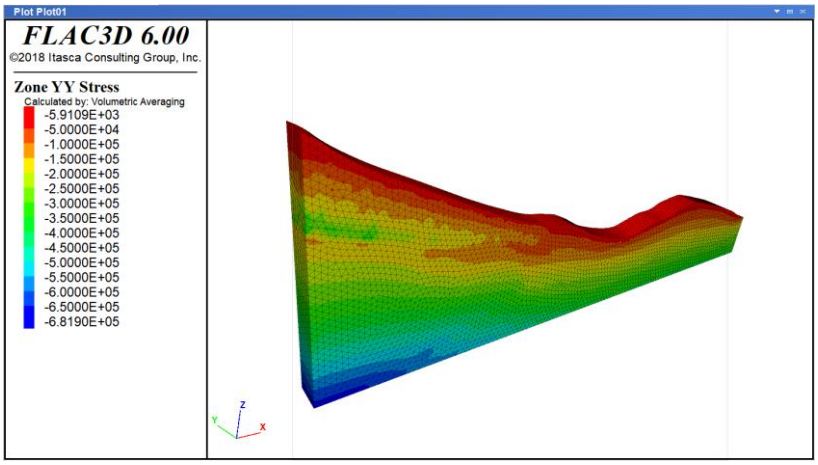

Fig. 2. Vertical stress cloud image of the original slope

The allocation of the maximum principal stress is shown in Fig. 8. The values of the maximum principal stress are all negative, indicating that all parts of the slope are under compressive stress. On the whole, the stress value increases with decreasing slope elevation, reaching a maximum value of 4.21 × 105 Pa at the bottom of the slope, indicating that the slope is mainly affected by stress in the vertical direction.

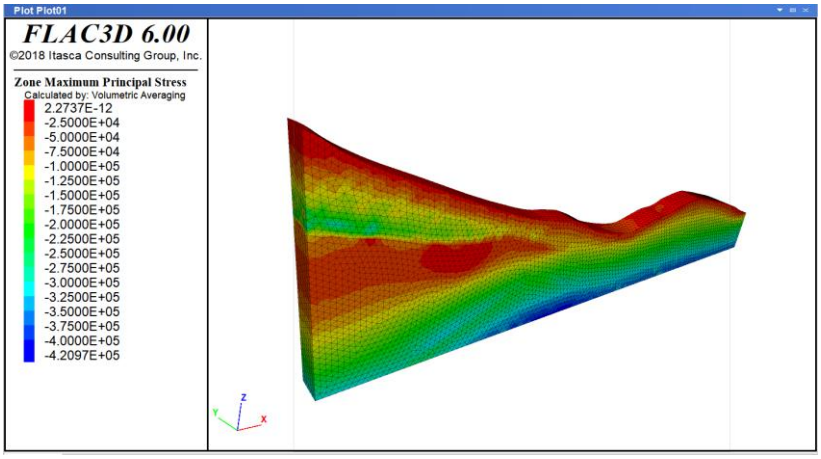

Fig. 8. Original maximum principal stress distribution diagram of the slope

3.4. REINFORCEMENT REQUIREMENTS

On the basis of the analysis performed using the limit equilibrium method and the strength reduction method, it can be seen that the slopes under the three different conditions face the

risk of landslides caused by instability. So it is urgent to manage the slope. According to the relevant requirements presented in the Landslide Prevention Engineering Exploration Code, the hazard level of the open-pit mine slope is Grade I. The safety factor of the reinforced slope should reach 1.30 under natural conditions, 1.20 under continuous rainfall conditions and 1.10 under seismic conditions, as shown in Table 4.

Table 4. Requirements of landslide safety factor under different working conditions

No.	Calculated conditions	Safety factor of anti-slip stability
1	natural conditions	1.30
2	rainstorm conditions	1.20
3	reismic conditions	1.10

4. SLOPE REINFORCEMENT STUDY

According to the above simulation results, the original slope is unstable under the three different conditions, among which the safety factor of the slope under rainstorm conditions is the lowest, with these being the conditions under which the slope is the most unstable. If the safety factor of slope under storm conditions is able to meet the requirements, the slope under natural and seismic conditions will also be able to reach a stable state. Because of the high risk of open-pit mine slope, deep reinforcements such as anchor reinforcement and anti-slide pile reinforcement were adopted. Therefore, these two schemes were studied below; the displacement of the slope was analyzed using numerical methods, and the parameters were optimized. With the aim of ensuring that the safety factor of the slope meets the requirements, the two optimized schemes were compared in order to select the best solution (Yang et al. 2015).

4.1. ANCHOR REINFORCEMENT SCHEME STUDY

4.1.1. OPTIMIZATION OF ANCHOR LENGTH

The anchor rod length is critical to the reinforcement measures and depends mainly on whether the end of the anchor rod crosses the slip surface. If the anchor rod is too short to cross the slip surface, it cannot provide sufficient tensile strength and cannot achieve the desired reinforcement effect; if the anchor rod is too long, it will be able to provide sufficient tensile strength, but will also be economically wasteful. The safety factor of the slope with anchor lengths between 18 m and 22 m was analyzed and the results compared. The relationship between anchor length and safety factor is shown in Fig. 9. The safety factor increases with increasing anchor length, and remains unchanged at lengths greater than 20 m. Therefore, in order to ensure the effectiveness of reinforcement measures and to not

cause economic problems such as material waste, the optimal anchor length was determined to be 20 m.

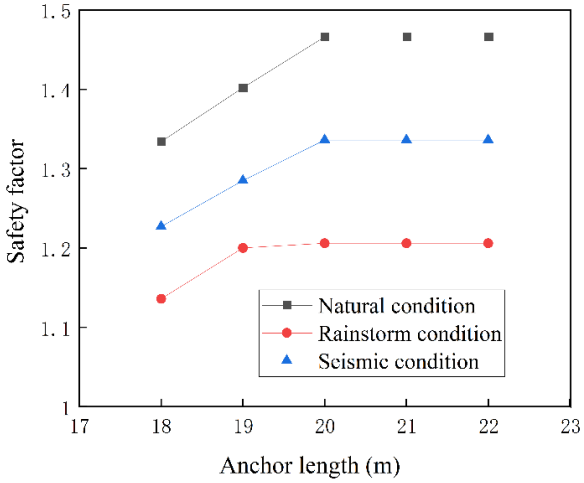

Fig. 9. Diagram of the relation between anchor length and safety factor

4.1.2. OPTIMIZATION OF ANCHORING ANGLE

The anchoring angle is a very important parameter in the design of anchor reinforcement. If the anchorage angle is too wide, the horizontal component force will be too small to achieve the expected reinforcement effect. Meanwhile, small anchoring angles can cause engineering problems such as grouting body settlement. Different anchoring angles can

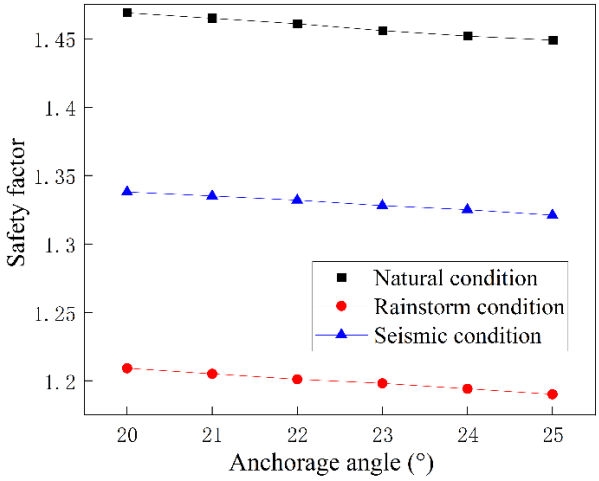

Fig. 10. Diagram of the relation between safety factor and anchorage angle

directly affect the slope support performance. The anchoring angle should not exceed 45°, and the best effect is achieved when the anchoring angle is between 20° and 25° (Xinrong 2015; Dong et al. 2020; Li et al. 2012). Therefore, the safety factor of the slope with anchorage angles in the range of 20°–25° was simulated and calculated. As shown in Fig. 10, the change characteristics of the safety factor of the slope under the three different conditions are consistent. With increasing achoring angle, the safety factor decreases, so the optimal angle was determined to be 20°.

4.1.3. OPTIMIZATION OF BOND LENGTH

Whether the anchor is effective also depends on the bond length of the anchor, so the safety factor of the slope with bond length ranging from 5 m to 10 m was simulated and studied. The results are shown in Fig. 11, where the safety factor increases continuously with increasing bond length. When the bond length is 9 m, the safety factor under storm conditions is 1.209, meeting the reinforcement requirements. The bond length of 10 m also meets the reinforcement requirements, but uses more material than a bond length of 9 m. In consideration of economic efficiency, the optimum bonding length of the anchor should be set as 9 m.

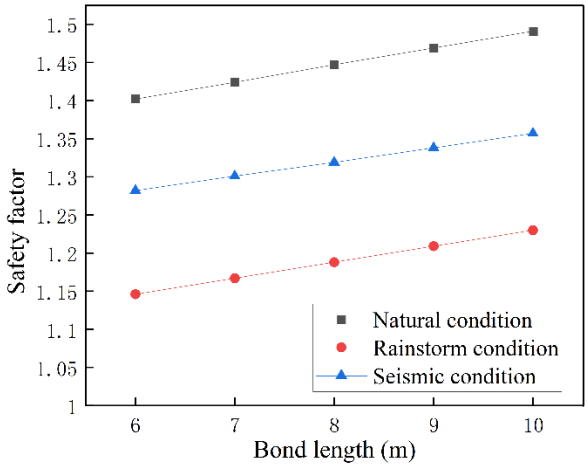

Fig. 11. Diagram of relation between safety factor and bond length

4.1.4. OPTIMIZATION OF ANCHOR SPACING

When designing an anchor reinforcement scheme, anchor spacing is an important element to be considered in order to ensure both economic efficiency and the improvement of safety factor. If the anchor rod spacing is too small, a group anchor effect will occur, and the anchor rods will influence each other, thus affecting the reinforcement effect of the anchor rods. If the anchor rod spacing is too wide, the pressure on individual anchor rods will be too high, leading to the destruction of anchor rods. Therefore, anchor rod

spacing should be reasonably determined, with the optimal anchor rod spacing being within the range 2-5 m (Tao 2013). On the basis of simulation, it was found that the safety factor of the slope under all conditions is able to meet the requirements when the spacing is 2 m. However, when the spacing is greater than 2 m, the safety factor is too low to meet the reinforcement requirements. Therefore, in this study, the anchor spacing was set as 2 m.

4.1.5. OPTIMIZATION OF ANCHOR ROW SPACING

Following optimization, parameters such as the anchor length and anchorage angle were determined. In addition, FLAC3D was then used to simulate the reinforced slope in order to study the stability of the slope with row spacings of 2 m, 4 m, 6 m and 8 m, respectively. The relationship between the row spacing and the safety factor of the slope is presented in Fig. 12. The results show that the four reinforcement schemes with different row spacings all result in a safety factor that meets the safety requirements. Increasing the row spacing of the anchor can reduce the economic cost, but with a consequent decrease in the safety factor and stability of the slope. In consideration of the safety factor and economic cost, it is also necessary to prevent the occurrence of excessive slope displacement and bolt failure. Therefore, it is necessary to analyze the displacement of the slope and the bolt to determine the optimal row spacing.

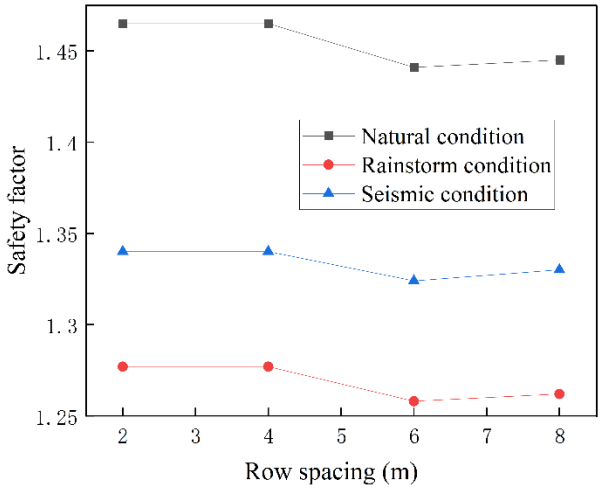

Fig. 12. Diagram of the relation between bolt row spacing and safety factor

The slope and anchor node displacement after reinforcement under the three working conditions with different row spacings were roughly similar. Taking the slope under continuous rainfall as an example, the slope and bolt displacement are shown in Fig. 13. A circular surface appears at the top of the slope, and the displacement of the part above

this surface is significantly larger than that of the surrounding soil, and the area of displacement change is obviously decreased compared with that before reinforcement.

The closer the anchor is to the slope surface, the greater the displacement, indicating that the load at the top of the anchor is greater than that at the bottom of the anchor. The closer the same row of anchors is to the middle of the slope, the greater the amount of displacement occurring, showing that the stress in the middle of the slope is greater than that at other parts, and the anchor rods are subjected to a greater load force.

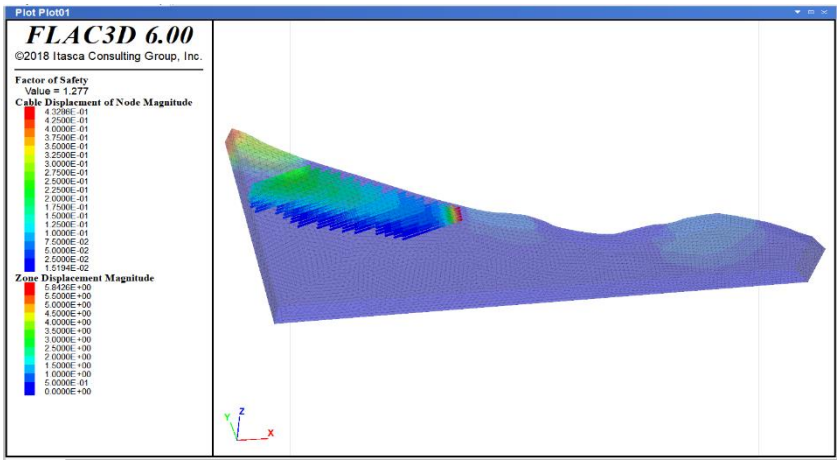

Fig. 13. Displacement distribution diagram of the slope and the anchor bolt

The peak displacements of slope and anchor nodes under the natural, rainfall and seismic conditions are summarized in Table 5, which shows that the peak displacements of the slope and anchor nodes are the smallest when the row spacing is 6 m.

Table 5. Peak displacement of the slope and anchor nodes with different row spacings

Row spacing	Peak displacement of slope [m]			Peak displacement of anchor nodes [m]		
	Natural conditions	Rainstorm conditions	Seismic conditions	Natural conditions	Rainstorm conditions	Seismic conditions
2 m	6.04	5.84	7.52	4.48	4.33	5.26
4 m	7.64	7.09	6.79	4.52	4.38	5.25
6 m	5.08	5.22	7.12	4.41	4.28	5.18
8 m	5.52	5.82	8.07	4.42	4.32	5.19

To ensure the stability of the slope, the safety factor should be increased as much as possible, meanwhile, the displacement of the anchor rod should be minimized to ensure that the anchor rod is not damaged. Considering the economic benefits, the row spacing should be 6 m for anchor rod reinforcement, not only guaranteeing the slope stability

and the effectiveness of the anchor rod, but also reducing the economic expenditure. The longitudinal depth of the slope is 10 m, and two rows are set with a row spacing of 6 m, with 16 anchors in each row and 32 anchors in total. The safety factor of the reinforced slope under different conditions is shown in Table 6, and the values obtained are able to meet the slope reinforcement design requirements.

Table 6. Safety factor of slope reinforced with anchor bolts with 6 m spacing

Conditions	Natural conditions	Rainstorm conditions	Seismic conditions
Safety factor	1.441	1.258	1.324

4.2. ANTI-SLIDE PILE REINFORCEMENT SCHEME STUDY

4.2.1. OPTIMIZATION OF THE NUMBER OF ANTI-SLIDE PILES

In the design of the anti-slide pile reinforcement scheme, the number of piles is one of the factors that must be considered. The greater the number of piles, the better the reinforcement effect will be. However, too many piles will only increase the economic cost, so the optimal number of anti-slide piles needs to be determined. Slopes with different numbers of piles were simulated, and the results are shown in Fig. 14. The results show that the safety factor of the slope under the three conditions showed an upward trend with increasing numbers of piles. When the number of anti-slide piles is four, the safety factor of the slope under the different working conditions is able to meet the reinforcement requirements. To avoid material waste and reduce unnecessary economic cost, the optimal number of anti-slide piles was determined to be four.

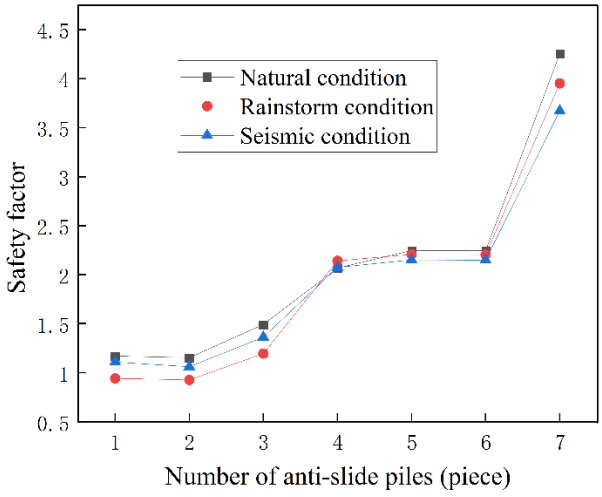

Fig. 14. Diagram of the relationship between safety factor and number of anti-slide piles

4.2.2. OPTIMIZATION OF THE SPACING OF ANTI-SLIDE PILES

After the determination of the number of anti-slide piles, the spacing of the anti-slide piles is also a factor that is necessary to consider. Spacings of anti-slide piles that are either too large or too small are not conducive to achieving the reinforcement effect. Therefore, the safety factor of the slope under different working conditions with pile spacings ranging from 15 m to 20 m was studied, and the simulation results are shown in Fig. 15. When the pile spacing is less than 18 m, the variation trend of the safety factor under different conditions is consistent, and increases with increasing pile spacing, but does not meet the reinforcement requirements. When the pile spacing is greater than 18 m, the changes in the safety factor under the three conditions are different. The safety factor under natural conditions first decreases and then increases; the safety factor under storm conditions shows a trend of first increasing and then decreasing; and the safety factor under seismic conditions shows a decreasing trend. According to the above simulation of the original slope, the safety factor under rainstorm conditions is the lowest, and the slope is the most unstable. Therefore, the design should be based on rainstorm conditions in order to maximize the safety factor of the slope under rainstorm conditions following reinforcement. Finally, a pile spacing 19 m was selected.

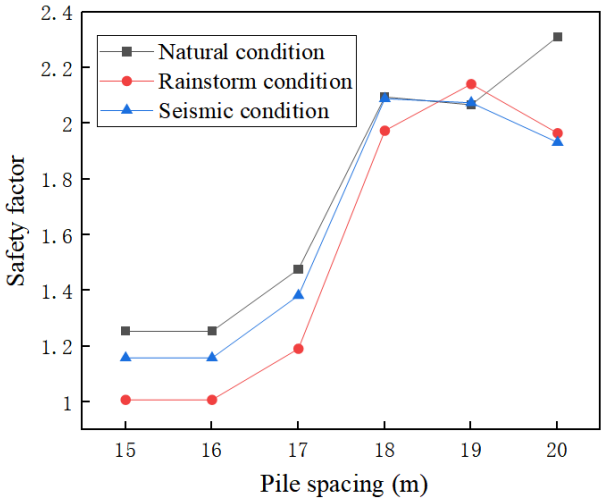

Fig. 15. Diagram of the relationship between pile spacing and safety factor

4.2.3. OPTIMIZATION OF THE ANTI-SLIDE PILE DIAMETER

In this study, cylindrical anti-slide piles were used for reinforcement, so the influence of the diameter of the anti-slide pile on the stability of the slope should be considered. If the diameter is too small, the safety factor will not be able to meet the requirements or provide reinforcement, while if the diameter of the pile is too large, it will result in

material waste and increased economic cost. The safety factor of the slope under different pile diameter conditions – 0.2 m, 0.4 m, 0.6 m, 0.8 m, 1 m, 1.2 m and 1.4 m – was calculated, and the results are presented in Fig. 16. The results show that the variation of the slope safety factor under the three conditions is consistent, and generally shows a trend that first increases and then slowly decreases. When the pile diameter is 0.4 m, the safety factor of the slope under various working conditions meets the reinforcement requirements. If the diameter continues to increase, this will only result in increased economic cost. Therefore, the optimal pile diameter was finally determined to be 0.4 m.

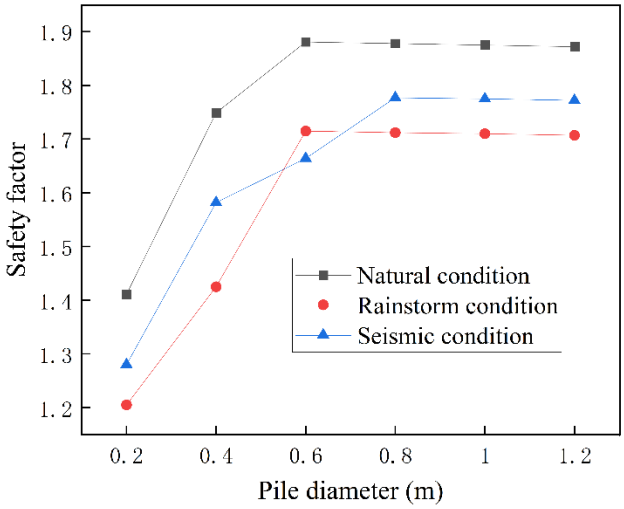

Fig. 16. Diagram of the relationship between pile diameter and safety factor

4.2.4. OPTIMIZATION OF ANCHORAGE DEPTH OF ANTI-SLIDE PILES

The depth of anti-slide piles in the subsurface is also one of the factors affecting the reinforcement effect. If the anti-slide pile is too short and does not cross the slip surface, it cannot perform its reinforcement role. If the anti-slide pile is too long, it will result in material waste and increase the economic cost. The lowest point of the anti-slide pile is determined on the same horizontal plane (i.e., the lowest elevation of each row of anti-slide piles is identical), and the anchorage depth and length of anti-slide piles are described by the lowest anchorage point elevation of anti-slide piles. The smaller the anchorage point elevation, the greater the anchorage depth of the anti-slide piles driven from the surface, and the longer the length of the anti-slide piles. The safety factor of the slope was simulated using different anchorage point elevations, and the results are shown in Fig. 17. The greater the anchorage point elevation, the smaller the anchorage depth of the anti-slide pile and the lower the safety factor. When the anchorage point elevation is greater than 38 m, the safety factor decreases to its minimum value and does not change anymore. When the elevation of the anchorage point is lower than 38 m,

the safety factor is able to meet the reinforcement requirements. Compared with 37 m, in the 35 m and 36 m cases, the length of anti-slide pile is longer, and the economic cost is higher. So the elevation of the anchorage point was determined to be 37 m.

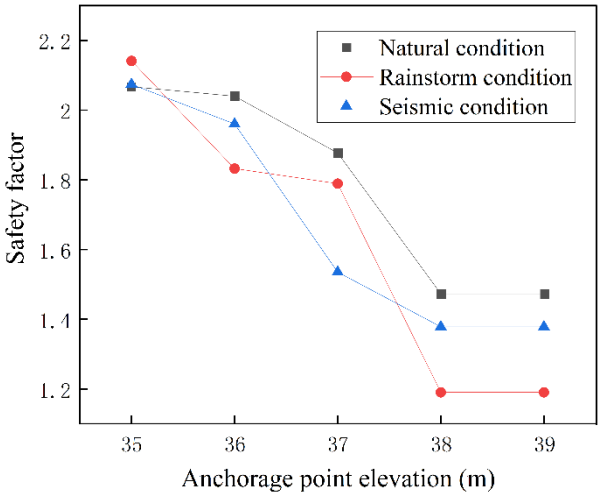

Fig. 17. Diagram of relationship between anchorage point elevation and safety factor

4.2.5. OPTIMIZATION OF ANTI-SLIDE PILE ROW SPACING

After the optimization of the anti-slip pile parameters, the simulation of the reinforced slope needs to be continued using FLAC3D in order to study the effect of different row spacings on the reinforcement effect of anti-slip piles, and the results are shown in Fig. 18.

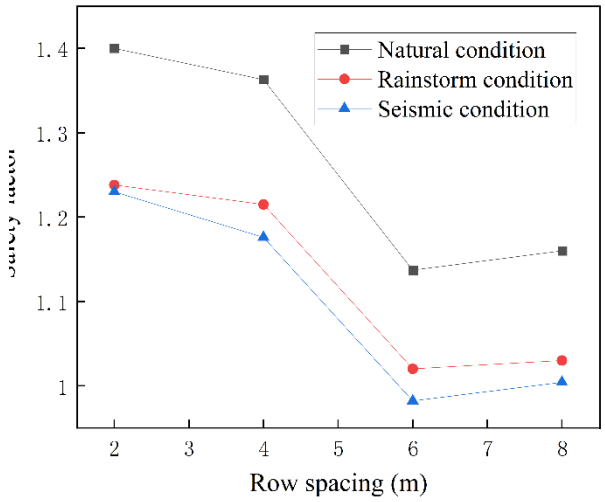

Fig. 18. Relation diagram of the distance between anti-slide pile rows and safety factor

With increasing row spacing distance, the safety factor shows a general decreasing trend. In addition, the safety factor of the slope at a row spacing of 6 m and a row spacing of 8 m does not meet the reinforcement requirements, so only row spacings of 2 m and 4 m need to be studied further.

Under different row spacings, the degrees of displacement of the slope and anti-slide pile nodes are roughly similar. The slope under continuous rainfall it taken as an example, as shown in Fig. 19. The displacement peaks of the anti-slide piles are all located at the top of the first row of anti-slip piles, and the displacement decreases from the top of anti-slip piles to the bottom. Similar to the anchor reinforcement scheme, the area where the peak displacement is concentrated is still the top of the slope, and the displacement decreases from the top to the bottom of the slope. However, when anti-slide piles are used for reinforcement, a new displacement change area appears in the middle of the slope, but the displacement change in this area has little effect on the overall stability of the slope.

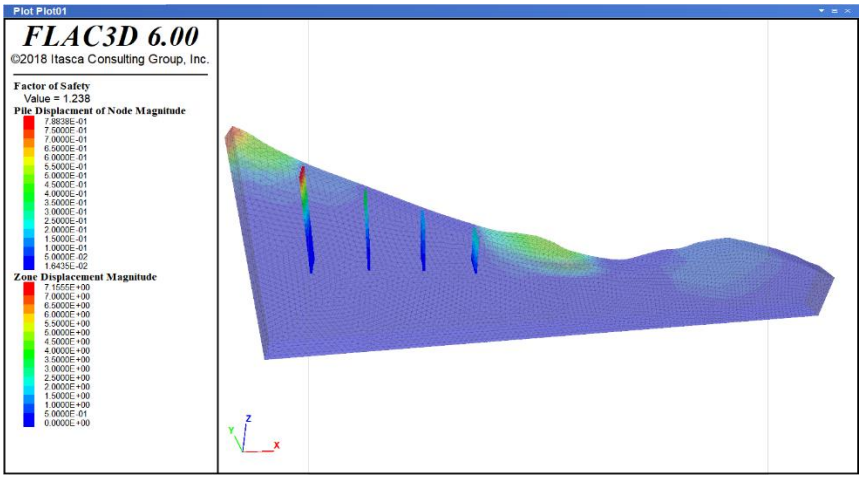

Fig. 19. Displacement distribution diagram of the slope and anti-slide piles

Table 7. Peak displacement of slope and anti-slide pile nodes with different row spacings

Row spacing	Peak displacement of slope [m]			Peak displacement of pile nodes [m]		
	Natural conditions	Rainstorm conditions	Seismic conditions	Natural conditions	Rainstorm conditions	Seismic conditions
2 m	6.87	7.16	10.84	0.76	0.79	0.96
4 m	21.92	20.42	29.43	2.99	3.42	6.61

The peak displacements of the slope and anti-slide piles under different working conditions are shown in Table 7. The peak displacement with a row spacing of 2 m is smaller than that with a row spacing of 4 m. The peak displacement of anti-slide piles with a row spacing of 2 m is at the decimeter level, while the peak displacement of anti-slip pile with a row spacing of 4 m is at the meter level, so the reinforcement effect is better with a row spacing of 2 m.

To ensure the stability of the slope, the safety factor of the slope should be increased. In addition, the displacement of the anti-slide piles should be reduced as much as possible in order to ensure that the anti-slide piles are not destroyed. Therefore, a row spacing of 2 m should be set for anti-slide pile reinforcement. When the longitudinal depth of the slope is 10 m and the row spacing is 2 m, five rows should be set with four anti-slide piles in each row, amounting to a total of 20 anti-slide piles. The different safety factors of the slope under different working conditions are shown in Table 8, where they are shown to meet the requirements of slope reinforcement.

Table 8. Safety factor of slope reinforced by 2 m row spacing anti-slide piles

Conditions	Natural conditions	Rainstorm conditions	Seismic conditions
Safety factor	1.4	1.238	1.23

4.3. COMPARISON OF THE REINFORCEMENT SCHEME BETWEEN ANCHOR AND ANTI-SLIDE PILE

In accordance with the optimal reinforcement scheme determined on the basis of the above simulation analysis, the anchor reinforcement scheme is more effective than the anti-slide pile reinforcement scheme, and the safety factor of the slope is relatively high. However, the safety factors of the slope under the two schemes are comparable, and both of them are able to meet the reinforcement requirements. With respect to economic considerations, 32 anchor rods are needed to implement the anchor reinforcement scheme, but only 20 anti-slide piles are needed to implement the anti-slide pile reinforcement scheme. Therefore, the anti-slide pile reinforcement scheme is more economical for ensuring the stability of slope.

5. CONCLUSIONS

Utilizing the site data of an open-pit mine slope, GeoStudio and FLAC3D were used to analyze the stability of the original slope and to propose a reinforcement plan; the following conclusions were drawn:

1. The GeoStudio and FLAC3D were used to simulate the original slope, and the safety factors solved by the different algorithms were similar, indicating a certain reliability. The results showed that the slope was in an unstable state under all three working conditions.
2. On the basis of the optimization of the anchor parameters, an anchor length of 20 m, an anchorage angle of 20°, a bond length of 9 m, an anchor spacing of 2 m, and a row spacing of 6 m were obtained. A total of 32 anchor rods were employed. The safety factors of the slope under the different working conditions were 1.441, 1.258 and 1.324, respectively.
3. On the basis of the optimization of the anti-slip pile parameters, an anti-slip pile number of 4, a pile spacing of 19 m, a pile diameter of 0.4 m, an anchorage point elevation of 37 m, and a row spacing of 2 m were obtained. A total of 20 anti-slide piles were required. The safety factors of the slope under the different working conditions were 1.4, 1.238 and 1.23, respectively.
4. By comparing the two schemes, on the premise of ensuring the effectiveness of slope reinforcement measures, combined with economic considerations, it is recommended to adopt the anti-slide pile reinforcement scheme.

ACKNOWLEDGEMENTS

The authors appreciate the financial support of project Nos. 51974015 and 51474017 provided by the National Natural Science Foundation of China; project No. SMDPC202101 provided by the Key Laboratory of Mining Disaster Prevention and Control (Shandong University of Science and Technology); project Nos. FRF-IC-20-01 and FRF-IC-19-013 provided by the Fundamental Research Funds for the Central Universities; project No. 2018YFC0810601 provided by the National Key Research and Development Program of China; project No. WS2018B03 provided by the State Key Laboratory Cultivation Base for Gas Geology and Gas Control (Henan Polytechnic University); and project No. E21724 provided by the Work Safety Key Lab on Prevention and Control of Gas and Roof Disasters for Southern Coal Mines of China (Hunan University of Science and Technology).

REFERENCES

XIAOMING G., 2010, *Study on Slope Reinforcement Design under Mining in Open Pit Mine*, Qingdao University of Technology.

VERMA D., THAREJA R., KAINTHOLA A. et al., 2011, *Evaluation of open pit mine slope stability analysis*, International Journal of Earth Sciences and Engineering, 4 (4), 590–600.

DENG C., 2021, *Research on multi-stage slope stability analysis method*, Lanzhou University of Technology Lanzhou.

AZMOON B., BINIYAZ A., LIU Z., 2021, *Evaluation of deep learning against conventional limit equilibrium methods for slope stability analysis*, Applied Sciences, 11 (13), 6060.

KAINTHOLA A., VERMA D., THAREJA R. et al., 2013, *A review on numerical slope stability analysis*, International Journal of Science Engineering and Technology Research (IJSETR), 2 (6), 1315–1320.

DENG D., ZHAO L., LI L., 2016, *Limit equilibrium method for slope stability based on assumed stress on slip surface*, Journal of Central South University, 23 (11), 2972–2983.

LI L., WANG Y., ZHANG L. et al., 2019, *Evaluation of critical slip surface in limit equilibrium analysis of slope stability by smoothed particle hydrodynamics*, International Journal of Geomechanics, 19 (5), 04019032.

ALEJANO L.R., FERRERO A.M., RAMÍREZ-OYANGUREN P. et al., 2011, *Comparison of limit-equilibrium, numerical and physical models of wall slope stability*, International Journal of Rock Mechanics and Mining Sciences, 48 (1), 16–26.

HARABINOVÁ S., 2017, *Assessment of slope stability on the road*, Procedia Engineering, 190, 390–397.

KALATEHJARI R., ALI N., 2013, *A review of three-dimensional slope stability analyses based on limit equilibrium method*, Electronic Journal of Geotechnical Engineering, 18, 119–134.

KUMAR V., BURMAN A., HIMANSHU N. et al., 2021, *Rock slope stability charts based on limit equilibrium method incorporating Generalized Hoek–Brown strength criterion for static and seismic conditions*, Environmental Earth Sciences, 80 (6), 1–20.

AGAM M.W., HASHIM M.H.M., MURAD M.I. et al., 2016, *Slope sensitivity analysis using spencer's method in comparison with general limit equilibrium method*, Procedia Chemistry, 19, 651–658.

TUTLUOGLU L., ÖGE I.F., KARPUZ C., 2011, *Two and three dimensional analysis of a slope failure in a lignite mine*, Computers & Geosciences, 37 (2), 232–240.

BUI H.H., FUKAGAWA R., SAKO K. et al., 2011, *Slope stability analysis and discontinuous slope failure simulation by elasto-plastic smoothed particle hydrodynamics (SPH)*, Géotechnique, 61 (7), 565–574.

LI D.Q., XIAO T., CAO Z.J. et al., 2016, *Efficient and consistent reliability analysis of soil slope stability using both limit equilibrium analysis and finite element analysis*, Applied Mathematical Modelling, 40 (9–10), 5216–5229.

YANG Y., TANG X., ZHENG H. et al., 2016, *Three-dimensional fracture propagation with numerical manifold method*, Engineering Analysis with Boundary Elements, 72, 65–77.

COETZEE C.J., 2017, *Calibration of the discrete element method*, Powder Technology, 310, 104–142.

FENGSHAN H., LEI W., 2016, *Application study of FLAC in analysis of slope stability*, Physical and Numerical Simulation of Geotechnical Engineering, (23), 17–23.

VYAZMENSKY A., STEAD D., ELMO D. et al., 2010, *Numerical analysis of block caving-induced instability in large open pit slopes: a finite element/discrete element approach*, Rock mechanics and rock engineering, 43 (1), 21–39.

NIAN T.K., HUANG R.Q., WAN S.S. et al., 2012, *Three-dimensional strength-reduction finite elementanalysis of slopes: geometric effects*, Canadian Geotechnical Journal, 49 (5), 574–588.

WEI W.B., CHENG Y.M., LI L., 2009, *Three-dimensional slope failure analysis by the strength reduction and limit equilibrium methods*, Computers and Geotechnics, 36 (1–2), 70–80.

VISHAL V., PRADHAN S.P., SINGH T.N., 2015, *An investigation on stability of mine slopes using two dimensional numerical modelling*, J. Rock Mech. Tunn. Technol, 21 (1), 49–56.

TSCHUCHNIGG F., SCHWEIGER H.F., SLOAN S.W. et al., 2015, *Comparison of finite-element limit analysis and strength reduction techniques*, Géotechnique, 65 (4), 249–257.

UTILI S., 2013, *Investigation by limit analysis on the stability of slopes with cracks*, Geotechnique, 63 (2), 140–154.

LESHCHINSKY B., AMBAUEN S., 2015, *Limit equilibrium and limit analysis: comparison of benchmark slope stability problems*, Geotech. Geoenviron. Eng., 141 (10), 04015043.

NADUKURU S.S., MICHALOWSKI R.L., 2013, *Three-dimensional displacement analysis of slopes subjected to seismic loads*, Canadian Geotechnical Journal, 50 (6), 650–661.

FAIZ H., YONG-GANG G., ALAM M. et al., 2020, *Stability Analysis of Slopes Based on Limit Equilibrium and Finite Element Methods for Neelum Jhelum Hydropower Project, Pakistan-Case Study*, American Journal of Engineering Research (AJER), 9 (3), 134–137.

LIU S.Y., SHAO L.T., LI H.J., 2015, *Slope stability analysis using the limit equilibrium method and two finite element methods*, Computers and Geotechnics, 63, 291–298.

YANG G., ZHONG Z., ZHANG Y. et al., 2015, *Optimal design of anchor cables for slope reinforcement based on stress and displacement fields*, Journal of Rock Mechanics and Geotechnical Engineering, 7 (4), 411–420.

XINRONG Z., LIXING L., 2015, *Solution of pre-stressed anchor arrangement parameters and slope safety factor*, Mineral Conservation and Utilization, (2), 18–21.

DONG M., ZHANG F., HU M. et al., 2020, *Study on the influence of anchorage angle on the anchorage effect of soft-hard interbedded toppling deformed rock mass*, KSCE Journal of Civil Engineering, 24 (8), 2382–2392.

LI X., HE S., WU Y., 2012, *Limit analysis of the stability of slopes reinforced with anchors*, International Journal for Numerical and Analytical Methods in Geomechanics, 36 (17), 1898–1908.

TAO Y., 2013, *Research and application of anchor support in slope stability problems*, Xi'an University of Technology, Xi'an.